



In-band LOS discovery using highly directional transceivers[☆]

Suman Bhunia^{a,*}, Mahmudur Khan^b, Murat Yuksel^b, Shamik Sengupta^c

^a Department of Computer Science, Texas A&M University, USA

^b Department of Electrical and Computer Engineering, University of Central Florida, USA

^c Department of Computer Science and Engineering, University of Nevada, Reno, USA



ARTICLE INFO

Article history:

Received 8 March 2018

Revised 17 November 2018

Accepted 28 April 2019

Available online 2 May 2019

Keywords:

Directional

RF

FSO

Line-of-sight

ad hoc

VANET

MANET

Discovery

ABSTRACT

Directional Radio Frequency (RF) / Free-Space-Optical (FSO) transceivers are envisioned to play a great role in future generation wireless networks. They provide benefits in terms of better throughput, enhanced spectrum utilization and lower interference from unwanted sources. However, the stringent requirement of line-of-sight (LOS) communication makes it tough for a mobile node to maintain a link without a-priori information about its neighbor's position. Hence, neighbor discovery takes a very crucial role in mobile ad hoc networks with directional transceivers. In this paper, we focus on neighbor discovery using highly directional transceivers operating on the same communication channel. We consider two nodes that can discover each other by steering their transceivers with a randomly chosen angular speed and performing a simple three-way handshaking protocol. We provide a theoretical analysis of the proposed neighbor discovery method. Additionally, we propose an algorithm where each node chooses its transceiver's angular speed and renews it if the neighbor is not discovered within an optimal time interval. We evaluate the proposed method via simulation as well as on a system prototype. Results from both simulations and experiments show the effectiveness of the proposed neighbor discovery protocol.

© 2019 Elsevier B.V. All rights reserved.

1. Introduction

Highly directional transceivers/antennas have attracted significant interest from telecommunication research and industry especially for ad hoc networks [2–5]. The high directionality of such transceivers provides higher gain, improves spatial reuse, and helps achieve higher data transfer rates. The transmissions from highly directional transceivers are harder to intercept and lowers the probability of jamming. All these advantages of directional antennas are suitable for tactical ad hoc networks where multiple entities desire to transmit high bandwidth data streams simultaneously [6–8].

As the radio frequency (RF) is becoming overcrowded, free-space-optical (FSO) communication is envisioned to play a crucial role in ad hoc networks as a complement of RF communication. Free-space-optical-communication (FSOC) not only provides the same advantages as communication using directional RF antenna but also makes high data rate point-to-point transfers possi-

ble. Both [9,10] has reported of achieving modulation speed of up to 10 Gbps. Moreover, FSOC uses the unlicensed optical spectrum which makes it cost efficient.

Despite the advantages provided by highly directional transceivers, they require maintenance of line-of-sight (LOS) between neighbors particularly for small wavelength bands such as FSO (infrared or visible) and millimeter-wave bands. The narrow beamwidth of these transceivers require very precise alignment between the transmitter and the receiver to establish a working communication link. So, a node has to steer its transceiver to face it towards the neighbor it wants to communicate with. Even if two nodes are within each other's communication range, they cannot communicate if their transceivers are not facing each other. In mobile settings, this may cause frequent link failures as a neighbor might move during the period when it is not being observed by a node. So, without having knowledge about the position of neighbors, a node can not communicate. Further, if two nodes are unaware of each others' position they have to find each other through neighbor discovery and exchange information about their trajectory in order to maintain directional links [11].

Various strategies have been proposed to maintain links between neighbors using directional antennas. All these methods consider the mode of operation to be half-duplex (HD) [2,4]. However, with the recent emergence of full-duplex (FD) communication technology, we are seeing a novel paradigm shift in wireless

[☆] The authors acknowledge partial support from NSF awards CNS #1663764 and CNS #1346600. A preliminary version of this paper has been published in the Military Communications Conference (IEEE MILCOM) 2016, Baltimore, USA [1].

* Corresponding author.

E-mail addresses: [sbhunias@tamu.edu](mailto:sbhunia@tamu.edu) (S. Bhunia), mahmudurk@knights.ucf.edu (M. Khan), мурat.yuksel@ucf.edu (M. Yuksel), ssengupta@unr.edu (S. Sengupta).

transceivers. Full-duplex operation provides enormous advancement for wireless networks where spectrum demands can be significantly reduced [12–16]. With full duplex transceivers in effect with directional antennas, it becomes interesting to see how mobile nodes can discover neighbors without using a redundant control channel.

In this paper, we focus on discovering a neighbor node without any prior knowledge about its location. We consider mobile nodes each with a highly directional FSO/RF transceiver mounted on a head/arm. The head/arm is mechanically steerable with which the FSO/RF transceiver can scan $2\pi^c$ (Here c denotes angle in radian). For smart RF transceivers/antennas with adaptive beamforming capability in high-frequency spectrum bands (such as mmWave), mechanical steering may not be required. These antennas are useful in short distance communication where range is not important but instantaneous switching between the beam directions is desired. However, adaptive beamforming antennas come with their own limitations such as lower-power, smaller accuracy in forming the desired beam pattern, and undesired sidelobes. Thus, in many applications, such as military flight communication where long distance communication is necessary but the beams are not required to shift with higher agility, directional antennas with fixed beamwidth are used [17,18]. These antennas are mechanically oriented towards the LOS. Recently, there has been a thrust on using mechanically steerable directional antennas due to their higher gain and narrower beam-form that is very useful for aeronautical communication [19–22].

We also assume that there is no GPS or omni-directional RF link available to synchronize or exchange location information. That is, we assume that the nodes operate in-band and use only the directional transceivers to discover each other. Both nodes operate in full-duplex mode. So, the proposed neighbor discovery scheme can be extremely useful in RF challenged environments and in scenarios where signal security is of utmost importance, for example, military robots like PackBots [23] can be equipped with highly directional transceivers. Such PackBots can be deployed in war-zones and they can discover each other by implementing the proposed scheme. The “In-band” communication and the high directionality of the transceivers prevents the possibility of RF interference and jamming by adversaries. Another potential application can be equipping autonomous vehicles operating in environments with few or no obstacles to LOS, like the NASA K10 robots [24] with such transceivers for Lunar/Mars exploration.

In the proposed neighbor discovery method, the nodes rotate their transceivers with randomly chosen angular speeds. Each node starts a three way handshake by sending a beacon message. Upon reception of a beacon, a node stops rotating and complete the handshake.

The main contribution of our work is to design and evaluate the first protocol that enables two neighbors with directional full duplex transceivers to discover each other. In particular, we:

- propose a method for nodes with directional transceivers to discover each other without any knowledge of neighbor’s location;
- propose a protocol that chooses angular speed randomly and reinstates the speed after a threshold time;
- prove that the proposed method helps discover a neighbor with high confidence within a small amount of time;
- demonstrate through extensive simulations that the proposed mechanism works well for both stationary and mobile setting;
- compare the proposed model with the state-of-the-art neighbor discovery scheme which shows that average neighbor discovery time can be lowered by 7 times;
- demonstrate that the model can be extended to discover multiple neighbors; and

- prove the feasibility of the proposed mechanism with a prototype developed using off the shelf hardware and electronic components.

The simulation results confirm that, with the proposed protocol, the average discovery time can be as small as 6s for mobile nodes with divergence angle of $\pi/36^c$ and 0.17s for mobile nodes with divergence angle of $\pi/5^c$. In The proposed model lowers the average neighbor discovery time by seven times when compared with the state-of-the-art neighbor discovery protocol presented in [25]. The system prototype evaluation shows that on average, the neighbor discovery takes 8.53s.

The rest of the paper is organized as follows: Section 2 surveys the relevant background on directional transmission and neighbor discovery. The proposed methodology, theoretical analysis and the algorithms are described in Section 3. Section 4 illustrates the simulation scenarios and discusses the results. Section 5 provides the details of a proof of concept prototype and its evaluation. Finally, Section 6 concludes the paper.

2. Background

In this section, we first discuss the motivation for directional transmission using both FSO and RF communications. Then, we present the existing neighbor discovery protocols that uses directional transceivers.

2.1. Directional transmission

In [10], a new technology involving FSOC between unmanned aircrafts (e.g., Aquila - UAV developed by Facebook) is proposed, that will help connect areas of the world that currently do not have Internet infrastructure. Methods for establishing and maintaining an FSO link among nearby balloons with the aid of GPS, RF, camera, and communication with a ground station are presented in [26,27], respectively. In both of these works, LOS alignment between the communicating nodes is first achieved using GPS information or using a camera to localize the neighbor node. During this phase, omni-directional RF communication is used. Only after locating the neighbor node, a pointing mechanism is used to align the FSO transceivers of the neighboring nodes. Then FSO is used only for exchanging data. The optical wireless link is not used for establishing or maintaining the link.

Unlike these out-of-band techniques, in [11], we proposed an in-band method that deals with the problem of maintenance of LOS alignment between two autonomous mobile nodes moving on 2D plane with mechanical steering of FSO transceivers. In [28], an in-band auto-alignment method for maintaining an FSO link between two unmanned aerial vehicles (UAVs) was proposed. For RF-challenged environments, such in-band techniques that only use the FSO link itself with no dependence on RF-based links are necessary.

2.2. Full-duplex transceivers

For RF transceivers, full duplex (FD) communication is achieved through active or passive self-interference suppression. In active interference suppression, a node cancels out its own transmitted signal received by its receiver by injecting a cancellation waveform in the direction of its own receiver antenna. In passive suppression, transmitter and receiver antennas are separated by an electromagnetic observer which enforces the signal strength at the receiver coming from its own transmitter to be below receiver cutoff [14]. For FSO transceivers, full duplex communication can be achieved by using transmitters and receivers of separate wavelengths [29,30]. Also, in-band full-duplex communication can be

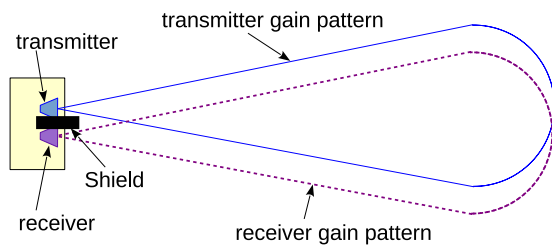


Fig. 1. Schematic diagram of a full duplex directional transceiver.

achieved via isolation of the transmitter and the receiver by placing a non-transparent material [31,32] between them or by using modulating retro-reflectors [33,34]. So, full duplex and/or directional operation on both RF and FSO transceivers have become possible and deserve a revisiting of some of the protocol designs in wireless systems. Fig. 1 illustrates the gain pattern of a full duplex FSO directional transceiver. Here, the transmitter and receiver are separated by a small distance and they face towards the same direction. A shield is placed to attenuate the feedback signal from the transmitter so that it does not reach the receiver.

Although full-duplex communication provides increased wireless channel capacity, it is prone to more interference compared to half-duplex communication. In [35], it has been shown that, even in the presence of interference, full-duplex communication can provide at least 20% gain over half-duplex communication. A new MAC protocol for full-duplex radio communication is proposed in [36] that helps achieve 88% throughput gain. Also, the effect of interference reduces significantly with increase in directionality of the transmitter and the receiver of a node [5].

2.3. Directional neighbor discovery

Neighbor discovery for directional RF has been well explored. Directional neighbor discovery protocols can be broadly classified into two categories: in-band and out-of-band. In out-of-band neighbor discovery, a separate communication channel (often achieved using an omni-directional antenna) is used to align the directional transceivers. In in-band neighbor discovery, no other communication channel is used.

The first category of mechanisms consider one omni-directional antenna and another directional antenna. Choudhury et al. [2,4], proposed a neighbor discovery protocol where the nodes can share their location information with each other using an omni-directional channel. Then, line-of-sight is established through transceivers with directional transmitters and omni-directional receivers. An and Hekmat [37] proposed a handshake based self-adaptive neighbor discovery protocol for ad hoc networks with directional antenna. This paper also considers directional transmitter and omni-directional receiver for neighbor discovery while frequency of operation is determined on the run. Ramanathan et al. [3] implemented an ad hoc network with directional antennas where the nodes are assumed to be synchronized through GPS clock cycle and utilizes an omni-directional channel to discover new neighbors.

Next, we discuss the neighbor discovery techniques using out-of-band communication channel where both the transmitter and the receiver are highly directional. Zhang and Li [5,38] proposed two algorithms for neighbor discovery with directional RF communication. The authors considered that the nodes are synchronized and use synchronized slots to transmit neighbor discovery requests. In a generic algorithm, each node transmits message with probability of 0.5 in random direction. In scan-based algorithm, nodes use a predefined scan sequence of antenna

direction. Although [5] provides a good analysis on number of slots required to complete the neighbor discovery, the consideration of all nodes using synchronous slots is not very practical. A node entering the network and not having any connectivity with any nodes in the network would not be able to synchronize its slots. Pei et al. [39] proposed another neighbor discovery protocol for directional MANETs based on synchronous search. The protocol assumes that all nodes are equipped with GPS for positional information and use wide bandwidth. Khan et al. [40] proposed a neighbor discovery method where the nodes rely on an omni-direction RF channel in addition to directional transceivers for initial synchronize among them.

Contrary to the schemes discussed above, some proposed mechanisms considered in-band communication for neighbor discovery. Vasudevan et al. [41] proposed a fully decentralized neighbor discovery method using highly directional antennas that does not require any prior information about the neighbors' locations. The protocol uses an optimal value of probability for transmitting beacon message at random direction. The protocol requires a node to have an estimate of the density of the network for setting up the transmission probability. Jakllari et al. [42] proposed a polling based MAC protocol for MANETs where all nodes are synchronized in terms of the polling slots. It allocates slots for discovering new neighbors when all nodes in a MANET points to random direction and advertise for neighbor discovery. It also provides a framework to compute neighbor discovery time. We assume no synchronization among nodes. Chen et al. [43] proposed a deterministic algorithm where the nodes scan the surrounding environment following sequences generated using unique identifiers. Wang et al. [25] proposed a similar method for discovering neighbors in a mmWave network where the nodes are not aware of each other's location. They also consider the concept of the nodes having unique identifiers to generate sequences to act either in transmission mode or reception mode. They consider continuous rotation of antennas as the scanning scheme and assume that all nodes scan at pre-configured speeds. Both [25,43] provide bounds on the worst case discovery times which is very commendable. But the average discovery times become larger for such deterministic methods.

In [1], we presented a preliminary version our work on the neighbor discovery algorithm considering nodes equipped with highly directional transceivers. We assumed that there is no out-of-band support like GPS or an extra communication channel. But, our proposed neighbor discovery method does not require the assumption of nodes having unique identifiers to generate scanning sequences or to decide the mode of operation (transmit or receive). The transceivers scan the surrounding environment with continuous rotation with a speed chosen from a given range and resets this speed after a threshold period of time is reached. The periodic reset of angular speed in our proposed method benefits in cases where the neighbor discovery time can be very high. We validated the effectiveness of our proposed method through simulations. In this paper, we extend the work by including the case for discovering multiple neighbors where we consider the effect of packet collision too. We also provide a comparison of the proposed neighbor discovery method with a state-of-the-art discovery scheme. We performed further evaluation of the proposed scheme through real test-bed experiments for both stationary and mobile scenarios using a prototype built using off-the-shelf hardware and electronic components.

3. Methodology

3.1. Problem statement and assumptions

We assume the following for our proposed model:

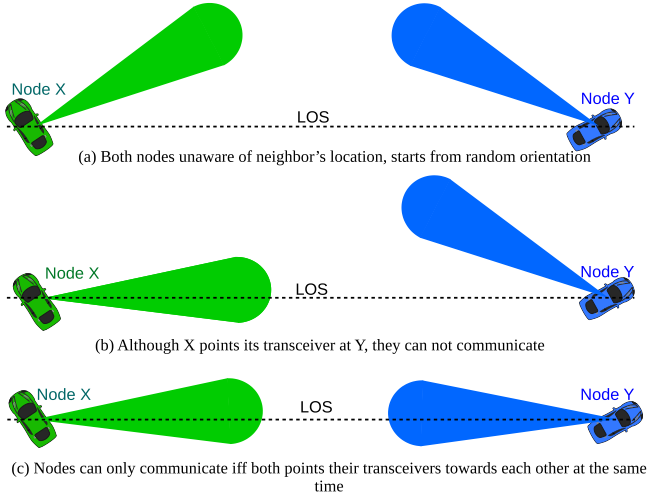


Fig. 2. Mandatory LOS for directional neighbor discovery.

1. *Full-duplex*: The communication between the nodes is full-duplex.
2. *In-band*: The discovery phase use in-band communication and does not require a separate control channel.
3. *Directional*: Both the transmitter and the receiver of a node face towards the same direction and rotate together as shown in Fig. 1. The receiver can receive signal from a neighbor that is within its main beam and the transmission beam of the neighbor must face towards the receiver (Fig. 2).
4. *Gain*: We consider that the nodes use highly directional transceivers with fixed beam width. We consider very high transmission gain in the direction of the main lobe and zero gain outside in the direction that is outside of main lobe.
5. *Transceiver rotation*: The nodes can rotate their transceivers using mechanically steerable heads. While performing neighbor discovery, both nodes rotate in the same manner (both clockwise/both counterclockwise).
6. *Asynchronous algorithm*: The nodes run the proposed algorithm in a distributed manner without any synchronization mechanism.

The proposed neighbor discovery protocol uses a three-way handshake for neighbor discovery (Fig. 3). A node rotates its transceiver at a randomly chosen constant angular speed and transmits a Beacon or Hello message. If a node receives a Beacon message from its neighbor, it stops rotating its transceiver and replies to the neighbor with a B-ACK message. The node receiving the B-ACK message also stops rotating its transceiver and replies with an ACK message to the neighbor denoting completion of neighbor discovery. The angular speed is chosen from an optimal range such that it is fast enough for quick neighbor discovery and slow enough to allow the three-way handshake to be complete. Also, the nodes reset this angular speed if neighbor discovery is not successful after a given period of time. Upon completion of neighbor discovery, the nodes move to link maintenance phase as proposed in our earlier work [44].

The proposed neighbor discovery protocol is not limited to any particular medium access control (MAC) protocol. The source address field of the beacon packet contains the sender's ID or address. For discovering a specific neighbor whose ID is already known, the beacon packet should contain that ID in its destination field. However, if the intended neighbor's ID is not known or a node is trying to discover multiple neighbors, the destination ID field is set to broadcast mode. Upon receiving a beacon, a receiver discards the beacon if the beacon is destined to another receiver

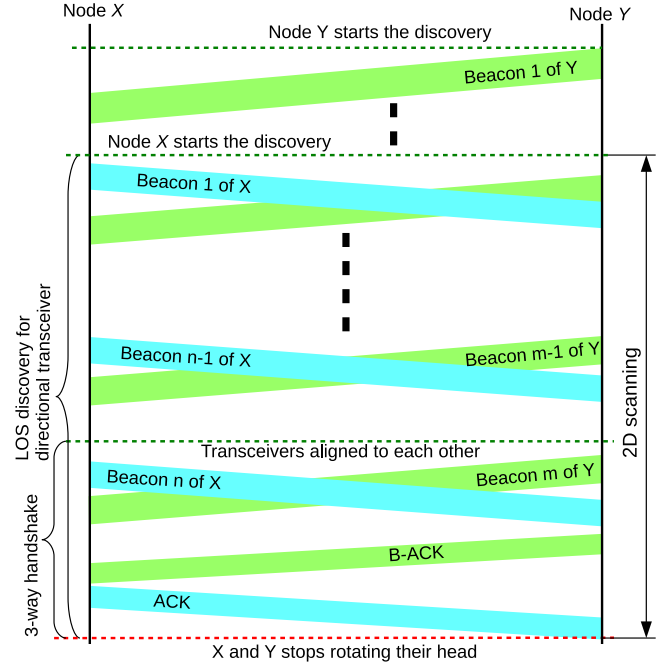


Fig. 3. Timing diagram of 3-way handshake for full duplex transceiver.

Table 1

List of used symbols.

Symbol	Description
β	Divergence angle of a transceiver
ω_x	Chosen angular speed of transceiver of node x
τ	Minimum time required to complete three-way handshake
θ_x	Initial angle at which x directs its transceiver
b_x^c	Beam border in clockwise direction
b_x^a	Beam border in anticlockwise direction
α	Chosen statistical confidence
T_α	Time required to have α confidence for neighbor discovery

or it does not desire to perform handshake with the sender of the beacon. If the beacon's destination field is set as broadcast address or the destination field matches with the receiver's address, the receiver sends the ACK packet immediately. Now, different MAC protocols will limit how quickly the ACK can be sent. WiFi-like MAC protocols enforce Short Inter-frame Space (SIFS) delay. This delay impacts on the three way handshake time. Our proposed methodology takes the three-way-handshake time (τ) as an input parameter alongside the transceiver's divergence angle (β) to calculate the rotational speed. If a MAC protocol enforces higher delay to the handshaking time, the rotational speed is reduced to provide sufficient time for the handshake.

3.2. Theoretical analysis

In this section, we investigate the probability of neighbor discovery within a bounded time. The used symbols are listed in Table 1. Let us consider that the total time required to send Beacon, receive B-ACK and then to send ACK is τ . It incorporates the transmission (t_{tran}), propagation (t_{prop}) and processing (t_{proc}) delays at both ends. τ can be calculated as:

$$t_{tran} = \frac{\text{Beacon size} + \text{B-ACK size} + \text{ACK size}}{3 \times \text{data rate}}$$

$$\tau = 3 \times t_{tran} + 3 \times t_{prop} + 2 \times t_{proc} \quad (1)$$

Now, t_{prop} will vary with distance but we can consider a maximum propagation delay as the time required for the signal to propagate

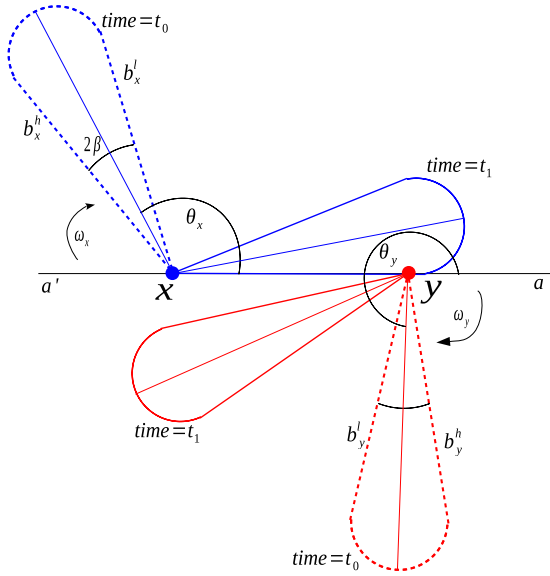


Fig. 4. Schema for neighbor discovery.

within transmission range which is in the order of nano seconds. t_{proc} can also vary depending on the hardware and the work load on the processor at that moment.

Theorem 1. For transceivers with divergence angle β and the handshake time τ , if the angular speed of either of the transceivers is greater than $2\beta/\tau$, neighbors cannot be discovered.

Proof. Let us consider the case of two stationary nodes x and y as depicted in Fig. 4. The main lobe is considered to be bordered by two angles namely lower border (b^l) which is the border in the clockwise manner and higher border (b^h) which is the border in the anticlockwise manner as shown in Fig. 4. A node can face its main lobe towards any direction $\theta \in [0^\circ, 2\pi^\circ]$. The beam borders are at a distance of divergence angle (β) from the normal of the lobe. We base our model with unit in radian denoted by $^\circ$. The mathematical model is equally valid for degree unit where π has to be replaced by 180° .

At time $t = t_0$, x is facing its transceiver at an angle of θ_x and y is facing its transceiver at θ_y . Now, we need to find out when x and y would be able to discover each other. It is obvious that the nodes can discover each other if at a certain time x and y both face their transceivers towards each other for at least τ amount of time. As it takes x 's beam $2\beta/\omega_x$ seconds to scan across y , the maximum angular speed for x should not be more than $2\beta/\tau$ so that the transceivers of x and y can hear each other for at least τ amount of time. As shown in Fig. 4, lower beam border of x , b_x^l , will reach aa' in $(\theta_x - \beta)/\omega_x$ seconds. Let's say l_x^n and h_x^n denotes the time when b_x^l and b_x^h respectively reaches the LOS axis aa' . Then:

$$l_x^n = \frac{(\theta_x - \beta) + 2n\pi}{\omega_x}; \quad n \in [0, 1, 2, \dots] \quad (2)$$

$$h_x^n = \frac{(\theta_x + \beta) + 2n\pi}{\omega_x}; \quad n \in [0, 1, 2, \dots] \quad (3)$$

Similarly, for y , the beam borders will reach aa' at:

$$l_y^m = \frac{(\theta_y - \beta) + (2m - 1)\pi}{\omega_y}; \quad m \in [0, 1, 2, \dots] \quad (4)$$

$$h_y^m = \frac{(\theta_y + \beta) + (2m - 1)\pi}{\omega_y}; \quad m \in [0, 1, 2, \dots] \quad (5)$$

Thus, the discovery can be completed if for any value of n and m , the following condition is satisfied

$$\min(h_x^n, h_y^m) - \max(l_x^n, l_y^m) \geq \tau \quad (6)$$

For successful neighbor discovery, the main beam of a node has to face its neighbor for at least τ time, i.e. $\forall_n h_x^n - l_x^n \geq \tau$. Replacing these values from (2) and (3), we can derive that $2\beta/\omega_x \geq \tau$. Thus $\omega_x \leq 2\beta/\tau$. Similarly, we can prove that $\omega_y \leq 2\beta/\tau$. Thus, they can not discover each other if any one of them has a angular speed greater than $2\beta/\tau$. \square

Theorem 2. If nodes x and y rotate their transceivers with same angular speed ω , then they can be discovered iff

$$\theta_x - 2\beta + \omega\tau \pm \pi < \theta_y < \theta_x + 2\beta - \omega\tau \pm \pi \quad (7)$$

where θ_x and θ_y are the initial orientation of nodes x and y w.r.t the LOS.

Proof. As shown in Fig. 4, $\theta_x^l = \theta_x - \beta$, $\theta_x^h = \theta_x + \beta$, $\theta_y^l = \theta_y - \beta$ and $\theta_y^h = \theta_y + \beta$.

Case I: $\theta_x + \pi < \theta_y$. Then, b_x^l will reach aa' before b_y^l does. Here, θ_x^l will reach aa' at $t = (\theta_x - \beta)/\omega$ seconds. θ_x^h will reach aa' at $t = (\theta_x + \beta)/\omega$ seconds. Then, θ_y^l has to reach aa' before $t = (\theta_x + \beta)/\omega - \tau$. So, $(\theta_y - \beta)/\omega < (\theta_x + \beta)/\omega - \tau + \pi$ or, $\theta_y < \theta_x + 2\beta - \omega\tau + \pi$.

Case II: $\theta_x + \pi > \theta_y$. Then b_y^l will be aligned with aa' before b_x^l . Then, θ_y^l must leave aa' only after $(\theta_x - \beta)/\omega + \tau$, which yields, $\theta_y > \theta_x - 2\beta + \omega\tau + \pi$. Thus, the condition for successful neighbor discovery is,

$$\theta_x - 2\beta + \omega\tau + \pi < \theta_y < \theta_x + 2\beta - \omega\tau + \pi$$

Similarly, we can prove that,

$$\theta_x - 2\beta + \omega\tau - \pi < \theta_y < \theta_x + 2\beta - \omega\tau - \pi$$

Consolidating these two equations will yield (7). \square

Lemma 1. The probability that the nodes discover each other increases as the t_{lcm} increases, where t_{lcm} is the Least Common Multiple (LCM) of the time required for each of the transceivers' full rotation.

Proof. The transceivers of nodes x and y will complete a circle in $2\pi/\omega_x$ and $2\pi/\omega_y$ seconds respectively. Both nodes will come to same formation after every $LCM(2\pi/\omega_x, 2\pi/\omega_y)$ seconds. So, we can say that the probability of discovery P_d is equal to the probability of discovery within t_{lcm} , p_{lcm} . Within this time, b_x^l will touch aa' n_x times where,

$$n_x = \left\lfloor \frac{t_{lcm}}{2\pi/\omega_x} \right\rfloor \quad (8)$$

where, $t_{lcm} = LCM(2\pi/\omega_x, 2\pi/\omega_y)$. Let us assume that at time t_1 , b_x^l touches aa' . If b_y^l can touch aa' within $\frac{2\beta}{\omega_x} - \tau$ time, then it can receive the beacon and complete the handshake. So, for a successful discovery b_y^l can be at most at $\pi + \omega_y(\frac{2\beta}{\omega_x} - \tau)$. Thus, we can write probability of discovery in the first rotation p_0 as

$$p_0 = \frac{\omega_y(\frac{2\beta}{\omega_x} - \tau)}{2\pi} \quad (9)$$

Since, within t_{lcm} time, the transceiver will rotate n_x times, it will have as many chances to complete the discovery. So, probability of discover in t_{lcm} can be written as:

$$p(t_{lcm}) = 1 - (1 - p_0)^{n_x} \quad (10)$$

where $p(t)$ is the probability of discovery within time t .

Combining (8)–(10), it is clear that if t_{lcm} is high then the probability of detection is high. \square

Corollary 1. Probability of discovery within time t can be approximated as:

$$p(t) = p(t_{lcm})^{\lfloor t/t_{lcm} \rfloor} + (1 - p(t_{lcm}))p(t') \quad (11)$$

Proof. As b_x^l will cross the same position every t_{lcm} , we can say that the probability of discovery within a time that is a multiple of the t_{lcm} will be same as p_{lcm} . Let us assume, after spending $t_{lcm} \times \lfloor t/t_{lcm} \rfloor$ time, node x will have t' time left for discovery. The number of full rotations of x within t' can be derived as:

$$n_{t'} = \left\lfloor \frac{t'}{2\pi/\omega_x} \right\rfloor \quad (12)$$

where, $t' = t - t_{lcm} \times \lfloor t/t_{lcm} \rfloor$. Then, probability of discovery within $n_{t'}$ rotation,

$$p_{n_{t'}} = 1 - (1 - p_0)^{n_{t'}} \quad (13)$$

Let us assume, after $n_{t'}$, there is t'' time left. Similar to (9), we can say that b_x^l can touch the aa' line anytime between 0 and $2\pi/\omega_x - \tau$. Thus, the probability of discovery within a time t'' where t'' is less time than a full rotation, can be derived as:

$$p_{t''} = p_0 \times \frac{t''}{2\pi/\omega_x}; \quad \tau \leq t' \leq 2\pi/\omega_x \quad (14)$$

where, $t'' = t' - \frac{2\pi}{\omega_x} \times n_{t'}$. Then we can calculate the probability of discovery in t' as:

$$p_{t'} = p_{n_{t'}} + p_{t''} \quad (15)$$

Since, probability of discovery in first $n_{t'}$ time is same as probability of discovery in first t_{lcm} , we can write, probability of discovery within time t can be written as (11). \square

3.3. Rotational speed reset time

A node randomly chooses its transceiver's rotational speed without any knowledge about its neighbor's location or rotational speed. Now, for some combinations of the rotational speeds of a pair of neighboring nodes, the discovery time can be very high (for an example if they choose equal speed). Therefore, if a node does not discover its neighbor within a given time period it resets its rotational speed.

Let $p_t(\omega_{\min}, \omega_{\max})$ be the probability of discovery within time t where ω_{\min} and ω_{\max} are the lower and the upper limit of choosing the angular speed ω_x and ω_y . Since having a strict range $(0, 2\beta/\tau)$ for choosing a rotational speed may not be optimal, the range is chosen as $[\omega_{\min}, \omega_{\max}]$ at the starting of the neighbor discovery phase. Let $\alpha \in (0, 1)$ be a statistical significance for neighbor discovery (i.e., the probability of neighbor not being discovered is α). Then under the base model assumption, we can find out the time required, T_α , to ensure the probability of neighbor discovery of at least $1 - \alpha$.

$$T_\alpha(\omega_{\min}, \omega_{\max}) = \min t \quad (16)$$

$$s.t. \quad P_t(\omega_{\min}, \omega_{\max}) \geq 1 - \alpha$$

Now, for a given α , the optimal values for T_α can be observed as:

$$T_\alpha^{opt} = \min_{\omega_{\min}, \omega_{\max}} T_\alpha(\omega_{\min}, \omega_{\max}) \quad (17)$$

$$s.t. \quad \omega_{\min} \in [0, 2\beta/\tau]$$

$$\omega_{\max} \in (0, 2\beta/\tau]$$

$$\omega_{\min} < \omega_{\max}$$

Now, from the optimal value of ω_{\min} and ω_{\max} are:

$$\omega_{\min}^{opt} = \arg \min_{\omega_{\min}} (T_\alpha(\omega_{\min}, \omega_{\max})) \quad (18)$$

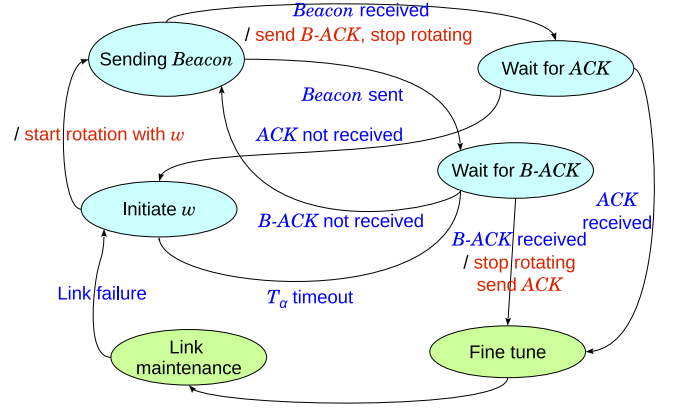


Fig. 5. State transition diagram.

$$\omega_{\max}^{opt} = \arg \min_{\omega_{\max}} (T_\alpha(\omega_{\min}, \omega_{\max})) \quad (19)$$

The mathematical model for obtaining $\mathbb{P}(\text{discovery})$ within a given time, resembles a continuous space markov chain as the initial position for the nodes are in $[0, 2\pi)$. We observed the effect of $\omega_{\min}, \omega_{\max}$ on T_α through rigorous simulations. The simulation results are discussed in Section 4.1.3.

3.4. Randomized neighbor discovery

Algorithm 1 presents the steps of neighbor discovery whereas Fig. 5 illustrates the state diagram of a node. The main idea behind this algorithm is to rotate the transceivers in a steady speed ω and if the neighbor is not discovered within a given amount of time then ω is changed.

Algorithm 1: Algorithm for neighbor discovery

- 1 Choose optimal confidence level α
- 2 Determine ω_{\min} and ω_{\max} from the optimal point
- 3 Choose an random angular speed $\omega \in (\omega_{\min}, \omega_{\max})$
- 4 $Timeout \leftarrow current_time + T_\alpha$
- 5 Start rotating the transceiver with ω
- 6 Send the Beacon
- 7 **if** Beacon received from other node **then**
- 8 | stop rotating and send B-ACK
- 9 **else if** B-ACK received from neighbor **then**
- 10 | stop rotating send ACK
- 11 | Start link maintenance phase
- 12 **else if** ACK received from neighbor **then**
- 13 | stop rotating and start link maintenance phase
- 14 **else if** $current_time > Timeout$ **then**
- 15 | Goto step-8
- 16 **else**
- 17 | Goto step-11

As the first step, a node chooses an optimal confidence level, α , given β and τ . The optimal value of α is observed through simulation described in Section 4.2. The node uses (17) to determine optimal values for ω_{\min} and ω_{\max} and randomly selects an angular speed from $(\omega_{\min}, \omega_{\max})$. At this point the node can forecast that within T_α seconds the neighbor can be discovered with a probability greater than $1 - \alpha$. A *timeout* value is set as the current time with addition to T_α . Now, the node starts rotating its

transceiver clockwise and sends beacon messages. Since we are considering full duplex communication, the node can receive beacon from the neighbor while transmitting beacons. If a beacon is successfully received from the neighbor node, it stops rotating its transceiver and sends an B-ACK message. Similarly, if B-ACK is received from a neighbor, it stops rotating and sends a ACK message to denote completion of the three-way handshaking. The node transitions to link maintenance phase after successful completion of the handshaking. If neither B-ACK nor a beacon is received, the node keeps transmitting beacon messages while maintaining the angular speed. If the handshaking procedure is not complete during the timeout interval, the node changes to a new rotational speed for the transceivers. This new rotational speed is again randomly picked from $(\omega_{\min}, \omega_{\max})$.

3.5. Discovering multiple neighbors

In oblivious neighbor discovery [43], a node is unaware of its neighbors' locations as well as the number of neighbors. During the neighbor discovery phase, the nodes refrain from normal communication with other nodes. Due to the randomness, our protocol cannot provide a guarantee whether or not a neighbor could be discovered within a certain amount of time. Thus, we need to put a specific limit on how long a node should remain in the discovery phase. Without knowing exactly how many neighbors there may be to discover, a node will remain in the discovery phase for an infinite amount of time. In a practical implementation, the discovery phase will have to be limited in time. One way of doing so could be based on an absolute time value which will be treated as the "discovery window". The larger the window the higher the probability of discovering all neighbors but at the cost of reduced actual data communication time. Further curbing of the discovery phase could be done by putting a limit on the maximum number of neighbors to be discovered. A node can stop the discovery phase either when the discovery window is complete or the maximum neighbor count is reached.

Algorithm 2 provides the procedure for discovering multiple neighbors. The algorithm can be initiated in two modes: (1) where the set of neighbors to be discovered is known; and (2) where a specific time limit is allotted for neighbor discovery. Similar to the neighbor discovery algorithm for single node discovery, a node keeps rotating with angular speed ω picked from the optimal $(\omega_{\min}, \omega_{\max})$ and sends discovery beacons continuously. Upon receiving a beacon from a neighbor, it replies a B-ACK message. If a B-ACK is received from a neighbor corresponding to previous beacon it sent, it replies an ACK. This ensures that three-way handshake is complete. Unlike the single node discovery, in multiple node discovery, a node does not stop its rotation upon completing an individual handshake. Instead, it records the angular position of a neighbor upon detection, and when all neighbors are discovered or the allotted time for discovery is over, it exits the discovery phase.

4. Simulations and results

In this section, we describe the simulations using Python and MATLAB to analyze the effectiveness of the proposed neighbor discovery algorithm. In the next section we present the prototype and experiment results with the prototype. For simulation, we considered both stationary (both nodes stationary) and mobile (one or both nodes mobile) scenarios. We assumed the nodes to be in the transmission range (100m) of each other. Different divergence angles ($\pi/60^c$, $\pi/36^c$, $\pi/24^c$, $\pi/15^c$) were considered for the simulations.

We consider the MAC layer frame structure of the nodes to be similar to that of WiFi. Fig. 6 illustrates the MAC layer frame structure

Algorithm 2: Algorithm for neighbor discovery

```

1 if neighbor set known then
2   | Targets  $\leftarrow$  Set of nodes to be discovered
3   | Discovered  $\leftarrow \emptyset$ 
4 else
5   | Discovery_timeout  $\leftarrow$ 
6   |   current_time + Alloted time for discovery
7   | Choose optimal confidence level  $\alpha$ 
8   | Determine  $\omega_{\min}$  and  $\omega_{\max}$  from the optimal point
9   | Choose an random angular speed  $\omega \in (\omega_{\min}, \omega_{\max})$ 
10  | Timeout  $\leftarrow$  current_time +  $T_{\alpha}$ 
11  | Start rotating the transceiver with  $\omega$ 
12  | Send the Beacon
13  | if (Beacon received from a node  $i$ )  $\wedge$  ( $i \notin$  Discovered) then
14  |   | send B-ACK to  $i$ 
15  | else if ACK received from  $i$  then
16  |   | Discovered  $\leftarrow \{i\} \cup$  Discovered
17  | else if B-ACK received from neighbor  $j$  then
18  |   | Send ACK to  $j$  Discovered  $\leftarrow \{j\} \cup$  Discovered
19  | else if
20  |   | (Discovered = Targets)  $\vee$  (current_time > Discovery_timeout)
21  |   | then
22  |     | Stop rotating
23  |     | Exit
24  | else if current_time > Timeout then
25  |   | Goto step-8
26 else
27  | Goto step-11

```

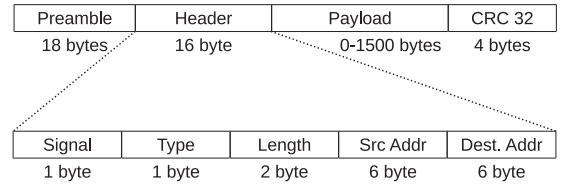


Fig. 6. MAC layer frame structure.

of the nodes, which is similar to that of WiFi. A frame consists of preamble, header, payload (data) and CRC field. For the three handshaking messages (Beacon, B-ACK and ACK) of the neighbor discovery protocol can be distinguished by the *Type* field of the header. For these three messages the payload size is zero. In this case, frame size is considered to be 38 bytes long. Considering 1 Mbps data rate, the transmission time for one packet is $304 \mu s$. Since, propagation delay is negligible compared to other delays, the value of τ can be determined from (1) as: $\tau = 3 \times 304 + 2 \times 100 = 1112 \mu s$.

4.1. Both nodes stationary

4.1.1. Obtaining statistical significance α

As the first step, we run a pilot simulation to see if neighbor discovery can be achieved within a short time with high confidence. Note that, here the nodes do not apply periodic reset of the angular speed. In every simulation, the nodes are initialized with their initial transceiver orientation randomly chosen from $[0, 2\pi)^c$. Also, each node randomly chooses its rotational speed from $[0, 2\beta/\tau)^c/s$. The simulation monitors when the two nodes discover each other. This simulation is repeated 1,000,000 times to obtain reliable results. Here, the packet processing time is

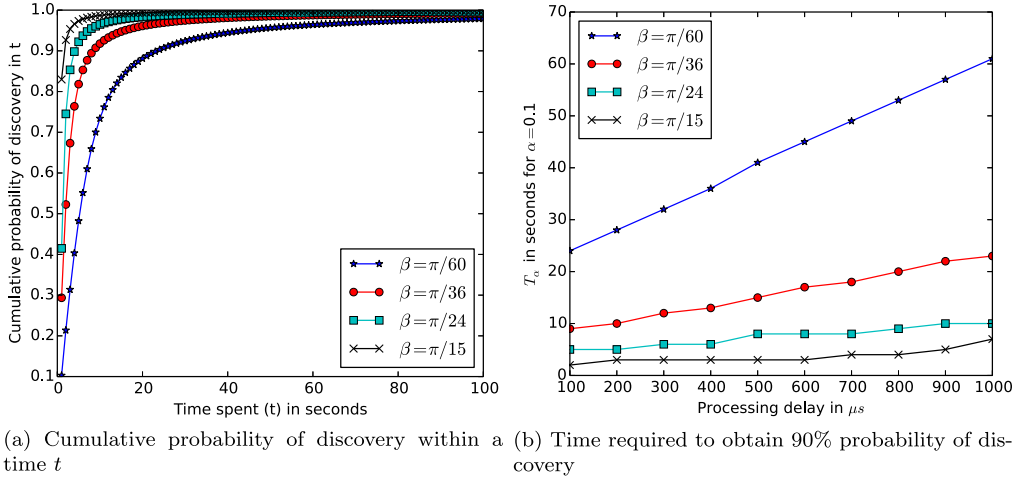


Fig. 7. (a) Cumulative probability of discovery within a time t (b) Time required to obtain 90% probability of discovery.

considered to be $100 \mu s$. Fig. 7 plots the probability of neighbor discovery within a given time. Here, x-axis represents time spent in seconds and y-axis represents the cumulative probability of neighbor discovery within time t . Four divergence angles of transceivers are being considered here. It is clear from the figure that the higher the divergence angle, the lower the amount of time is required for neighbor discovery. Note that, for some cases the neighbor discovery might never happen (for example if both the nodes choose same angular speed). In this case, the time taken for discovery will be ∞ . Thus, the cumulative distribution function will never reach 1. We can see that the neighbor can be discovered with a probability > 0.9 within a short period of time. However, to obtain a discovery probability of 0.95, a node needs significantly longer period of time. This necessitates the periodic reset of the angular speed.

4.1.2. Effect of packet processing delay

Fig. 7 depicts the effect of packet processing delay on the performance of the neighbor discovery protocol. Here, x-axis represents the processing delay in μs and y-axis represents the rotational speed reset time that is required to obtain 0.1 confidence ($T_{0.1}$), i.e. neighbor discovery probability of 0.9. For each set of parameters the simulation is repeated 1,000,000 times to obtain reliable results. At each simulation a node chooses an angular speed, $\omega \in (0, 2\beta/\tau)$, where τ is calculated according to (1). We can clearly see that for a very narrow beam transceiver ($\beta = \pi/60$), an increase in the processing time significantly increases the reset time; thus, increasing the neighbor discovery time. For transceivers with wider beam ($\beta = \pi/36^c$ or $\pi/24^c$ or $\pi/15^c$), the increase in reset time as the processing delay increases is less significant.

4.1.3. Choosing optimal ω_{\min} and ω_{\max}

Fig. 8 illustrates the effect of choosing different range of the angular speed. Here the results are plotted for two different values of divergent angle and three different ranges of the angular speed. It is very clear from the picture that choosing a hard range of $(0, 2\beta/\tau)$ does not provide optimal result as probability of discovery is lower in this case than that for the range of $(0.25 \frac{2\beta}{\tau}, 0.75 \frac{2\beta}{\tau})$.

In this section, the simulation is intended to obtain optimal values of ω_{\min} and ω_{\max} as a function of β , τ and α . The processing time is $100 \mu s$ and τ is calculated as in (1). Simulations are performed with different values of α . Fig. 9 presents the relationship between the range of angular speeds ($\omega_{\min}, \omega_{\max}$) and the time required for neighbor discovery with probability of 0.95 or $\alpha = 0.05$. Note that, in this plot both ω_{\min} and ω_{\max} are chosen from

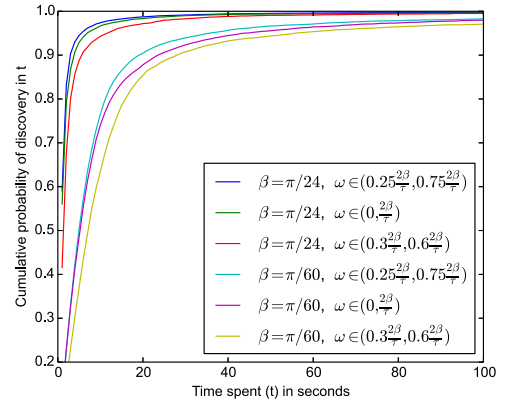


Fig. 8. Example of the effect of different ω_{\min} and ω_{\max} .

Table 2
 T_{α}^{opt} in seconds for different α and β .

α	T_{α}^{opt}			
	$\beta = \pi/60$	$\beta = \pi/36$	$\beta = \pi/24$	$\beta = \pi/15$
0.1	19.0	7.0	3.0	2.0
0.09	20.0	8.0	4.0	2.0
0.08	22.0	8.0	4.0	2.0
0.07	25.0	9.0	4.0	2.0
0.06	29.0	10.0	5.0	2.0
0.05	33.0	12.0	6.0	3.0
0.04	40.0	15.0	7.0	3.0
0.03	51.0	20.0	9.0	4.0
0.02	74.0	28.0	13.0	5.0
0.01	100.0	51.0	23.0	10.0

$[0, 2\beta/\tau]$. The results demonstrate that T_{α} is a concave function with respect to ω_{\min} and ω_{\max} . We found that $\omega_{\min} = 0.25 \times 2\beta/\tau$ and $\omega_{\max} = 0.75 \times 2\beta/\tau$ provides the optimal point (T_{α}^{opt}). Table 2 provides the obtained T_{α}^{opt} for different values of α and β .

4.1.4. Benefits of periodic angular velocity reset

So far, we have discussed how we can determine the period T after which nodes should reset their angular velocities. In this section, we compare the scenarios where the nodes use periodic reset and where they do not. In Fig. 10, we demonstrate the cumulative probability of discovery within a given time t . Simulations are carried out with the same parameters as before. The nodes chose random angular speed from $[\omega_{\min}, \omega_{\max}]$ and direction to start with.

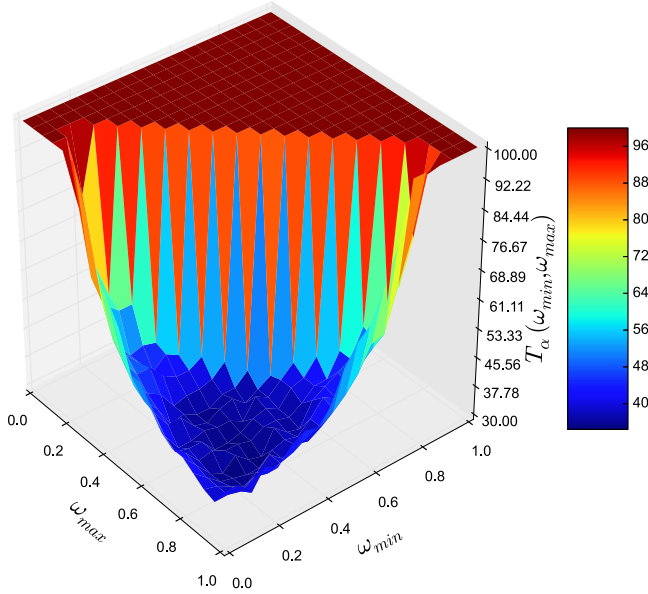


Fig. 9. Depiction of optimal T_α for $\beta = \pi/60$.

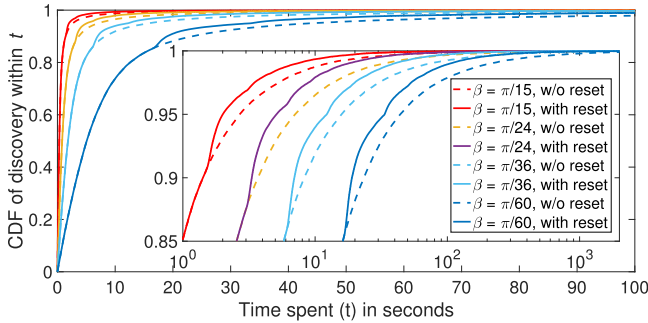


Fig. 10. Advantage of periodic reset. The outer graph depicts the cumulative probability of discovery within time (t). For better viewing we trim the time to 100 s in the outer figure. To better visualize the effect of the reset, in the inner graph, we elongated the time to 1000s where X-axis is in log-scale.

For the simulations with periodic reset, we use the T_α^{opt} as obtained from Table 2 for $\alpha = 0.05$. Note that if two nodes chose almost same angular velocities, chances are that they would not be able to discover each other within a small time period. Thus, the cumulative probability of discovery increases with the time provided, but it does not reach 1. We have zoomed the prominent portion in the inner plot to visualize the differences in more detail. In the inner subplot, we can see that for a divergence angle of $\pi/60$, the CDF reaches 0.88 at time $t \approx 20$ s, however with periodic angular velocity reset at every T_α , the CDF gets increased to 0.91. Although neighbors are discovered quickly most of the time, there are a few number of cases for which the neighbor discovery takes longer. The periodic reset of angular speed is particularly beneficial for these scenarios.

4.2. Both nodes mobile

Here, we consider both nodes to be mobile. The nodes' initial positions, speed (between 0-2.5 m/s) and transceiver orientation are randomly chosen. The divergence angle β is chosen as $\pi/36$. The simulator assumes a packet processing delay of $100 \mu\text{s}$. The transceivers use Algorithm 1 for discovering the neighbor. Note that T_α^{opt} is chosen from Table 2 and used as the rotational speed reset time. The simulation results are plotted in Fig. 11. Here x-axis

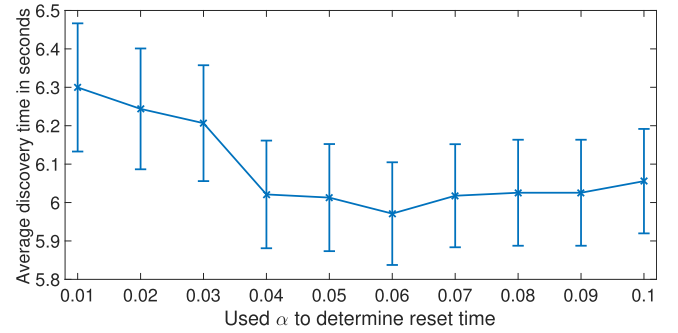


Fig. 11. Average discovery time for mobile nodes with $\beta = \pi/36$.

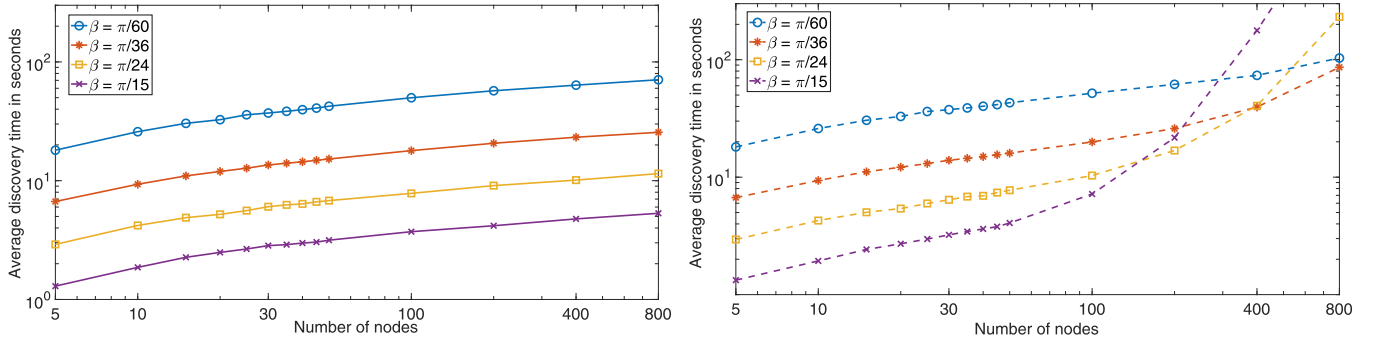
denotes the chosen confidence level α and y-axis denotes the average time required to complete neighbor discovery. The figure also depicts 95% confidence interval of the time required for neighbor discovery. It can be observed from the figure that at $\alpha = 0.06$, the average neighbor discovery time is the lowest. So, for $\beta = \pi/36$ and processing delay of $100 \mu\text{s}$, the optimal $\alpha = 0.06$.

4.3. Discovering multiple neighbors

We extended the evaluation of the proposed method further by performing simulations considering the discovery of multiple neighbor nodes. In this scenario, we varied the number of neighbor nodes, all other parameters are kept same as in Section 4.2. We do not consider gossip-based neighbor discovery, where, if two nodes X and Y discover each other, and two nodes X and Z discover each other then X can convey the location information of Y and Z. In this way, Y and Z can find themselves very fast. In our simulations, each node discovers its neighbors using only the method described in Algorithm 2.

If the network is densely populated and/or the nodes use wider beam, a node might have multiple neighbors within its beam coverage at a particular direction. Since our proposed neighbor discovery method does not employ any collision avoidance scheme, if these neighbors direct their transceivers towards the same node and transmit simultaneously, the packets will collide. So, a node will not be able to discover multiple neighbors located in such a manner within the same sweep. But, since the nodes change their transceiver rotation speed every T_α time, a node will be able to discover multiple neighbors located at the same direction on different sweeps.

We have conducted additional simulations considering the effect of packet collision. Fig. 12b displays the average discovery time. We can observe that, for smaller transceiver divergence angles β (e.g., $\pi/60^\circ$, $\pi/36^\circ$), the effect of packet collision is not very significant. For example, in a network of 400 nodes using $\beta = \pi/60^\circ$, a node can discover its 399 neighbors in 63.75s (Fig. 12a) when packet collisions are ignored, and in 73.5s (Fig. 12b) when packet collisions are considered. We can also observe that, the effect of packet collisions becomes severe for larger divergence angles such as $\beta = \pi/24^\circ$ or $\pi/15^\circ$. For instance, in a densely populated network of 400 nodes and $\beta = \pi/15^\circ$, the average discovery time for a node to discover its 399 neighbors is 177.7 s considering packet collisions and 4.768 s without considering collisions. We can observe that, for $\beta = \pi/15^\circ$, the average discovery time is even higher than that for $\beta = \pi/60^\circ$ when packet collisions are considered. So, for a smaller network size (e.g., < 200 nodes in Fig. 12b), larger transceiver divergence angles will provide better performance in terms of average discovery time. And, for a network with higher number of nodes, comparatively smaller divergence will result in lower discovery times.



(a) Results ignoring packet collisions (both axis in log-scale)

(b) Results considering packet collision (both axis in log-scale)

Fig. 12. Simulation results for discovering multiple neighbors.

4.4. Comparison with state-of-the-art scheme

As mentioned earlier, most of the prior work consider half-duplex (HD) mode of operation for neighbor discovery. In this paper, we consider the transceivers to be capable of full-duplex (FD) communication. But, our proposed neighbor discovery algorithm also works when the transceivers are in HD mode. In the HD scenario, a node alternates between transmission and reception modes. We assumed each node to be in transmission mode for T_{tx} amount of time and in reception mode for T_{rx} amount of time. Here $T_{rx} = t_{tran} + 2t_{prop} + t_{proc}$. Assuming very small propagation time t_{prop} (in the order of ns) compared to transmission time t_{tran} and processing time t_{proc} (in the order of $100 \mu s$), the equation can be written as $T_{rx} = t_{tran} + t_{proc}$. Considering two nodes A and B, for successful transfer of a packet, when A is in transmission mode, B must be in reception mode or vice versa. So, we can present the probability of successful transfer of a packet $P(ST)$ as:

$$\begin{aligned}
 P(ST) &= P(A \text{ in transmission and B in reception}) \\
 &\quad + P(B \text{ in transmission and A in reception}) \\
 &= 2 \times P(A \text{ in transmission}) \times P(B \text{ in reception}) \\
 &= 2 \times \frac{T_{tx}}{T_{tx} + T_{rx}} \times \frac{T_{rx}}{T_{tx} + T_{rx}} \\
 &= 2 \times \frac{t_{tran}}{2 \times t_{tran} + t_{proc}} \times \frac{t_{tran} + t_{proc}}{2t_{tran} + t_{proc}} \\
 &= \frac{2t_{tran}(t_{tran} + t_{proc})}{(2t_{tran} + t_{proc})^2} \quad (20)
 \end{aligned}$$

Using the values $t_{tran} = 305 \mu s$ and $t_{proc} = 100 \mu s$, $P(ST) \approx 0.48979$.

We also compare our proposed neighbor discovery scheme with the state-of-the-art method namely, hunting-based directional neighbor discovery algorithm (HB) [25]. In this method, each node continuously rotates its transceiver to scan for neighbors. The speed of angular rotation is chosen in such way to maximize the probability of discovery. Angular speed, while in transmission mode and reception mode are different. A node stays in transmission mode for enough time that ensures discovery if the other node is in reception mode. Each node is assumed to have a unique identifier, which is used to determine when to switch from transmission to reception mode and vice versa. In this work, packet processing time was not considered while calculating neighbor discovery times and two-way handshake method was assumed. For fair comparison, we consider three-way handshake and non-zero

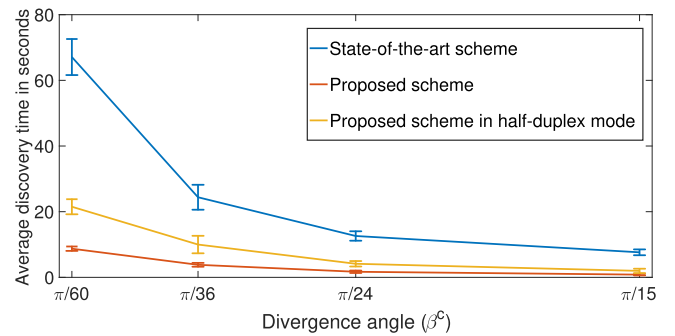


Fig. 13. Comparison of average neighbor discovery time with the state-of-the-art mechanism [25].

transmission and processing times in the simulations for both HB and FD.

4.4.1. Comparing average neighbor discovery time

In Fig. 13, we compare the average neighbor discovery times achieved using our proposed algorithm with those achieved using HB. We also compare the performance of our algorithm using half-duplex (HD) mode and full-duplex mode (FD). We can observe that, our proposed algorithm performs better using full-duplex mode (FD) than half-duplex mode (HD). For example, when $\beta = \pi/15^\circ$, average discovery time is 1.9667s for HD and 0.8290s for FD. Also, we can see that, the average discovery times achieved using our algorithm is less than those achieved using the state-of-the-art method.

4.4.2. Comparison of worst case performance

The state-of-the-art protocol provides a bounded time neighbor discovery, i.e. it guarantees that two nodes would be able to discover themselves within a threshold time. We recreated the scenarios and determined the bounded time in Table 3. We then provided the probability of neighbor discovery for our proposed scheme in full duplex and half duplex modes. We can clearly observe that within this bounded time, the probability of missed neighbor discovery is close to zero < 0.00015 .

To visualize the performance even more, we plotted the worst case neighbor discovery in Fig. 14. In this plot, we repeated the simulations for 100,000 times. We compare the worst case neighbor discovery time of [25] with the time required to discover neighbor with a probability of 99% and 99.9%. We can clearly see that the time required to discover neighbor with a confidence of

Table 3
Comparison of neighbor discovery time.

Divergence angle	Worst case discovery time for the state-of-the-art protocol [25]	Probability of discovery within this time using our full-duplex	Probability of discovery within this time using our half-duplex
$\pi/60$	3548.8 s	99.996%	99.987%
$\pi/36$	1815.33 s	99.997%	99.990%
$\pi/24$	684.39 s	99.993%	99.987%
$\pi/15$	421.47 s	99.997%	99.991%

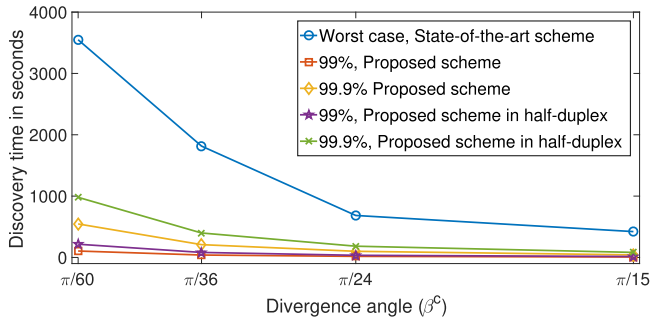


Fig. 14. Comparison of the worst case neighbor discovery time of [25] with the time required to discover neighbor in the proposed mechanism.

99% is much lower compared to the worst case performance of the state-of-the-art protocol.

5. Experimental evaluation

We have evaluated the effectiveness of our mechanism using a prototype built using off-the-shelf hardware and electronic components. In this section, we describe the system architecture of the prototype and present the experimental evaluation of our directional neighbor discovery method. For reader's convenience, a video demonstration depicting the prototype functionality is presented in [45].

5.1. System architecture

We had designed and built a prototype of the mobile node with a mechanically steerable FSO transceiver for our earlier work in [46]. We use the same prototype to perform experimental evaluation of the proposed neighbor discovery protocol. A brief description of the prototype is provided in this section. A detailed description of the original prototype can be found in [46].

We used commercially available off-the-shelf electronic components to build the prototype of the mobile node. Fig. 15 shows the block diagram of the prototype system architecture and Fig. 16 shows the different parts of the prototype, which are: a robot car, a mechanically steerable head, and an IR transceiver. These parts are controlled by a Raspberry Pi [47] using separate threads: head control, car control, and transmit or receive data.

5.1.1. Robot car and steerable head

We used the Emgreat 4-wheel Robot Smart Car Chassis Kits car [48] as the mobile node. The car is four-wheel drive with dimensions 25×15 cm and has carrying capacity of about 1kg. Its maximum speed is 40m/min. There are four motors each attached to a wheel that propel the car forward. The gate of a MOSFET is connected to a General-Purpose Input-Output (GPIO) pin on the Raspberry Pi where a pulse width modulated (PWM) signal is sent. By varying the duty cycle of this signal, the rotational velocity of the wheels can be controlled. As the steerable head, we used the Aluminum Robot Turntable Swivel Base [49], on which we mounted the IR transceiver. It is run by a servo motor. The swivel base consists of two rings, an outer ring, to which the servo is bolted to,

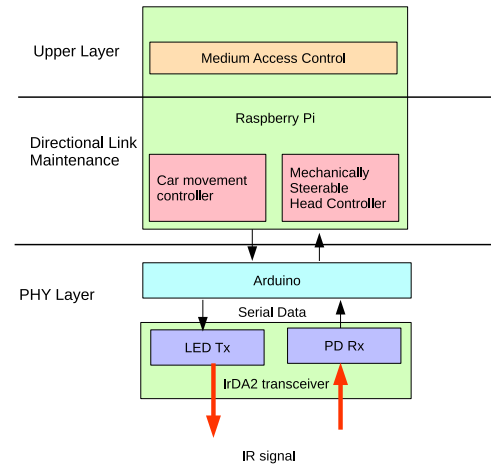


Fig. 15. Prototype system architecture block diagram.

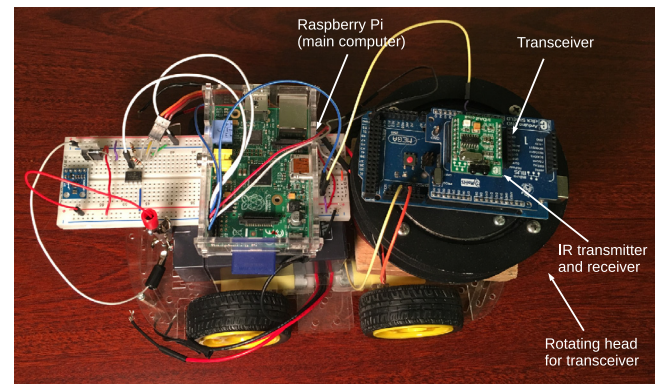


Fig. 16. Bird's eye view of the prototype.

and an inner ring, on which the gear is mounted, allowing for its controlled rotation. An op-amp was added to amplify the PWM signal from the Raspberry Pi GPIO pins, to achieve the required high voltage signal to run the servo motors.

5.1.2. Transceiver circuit

We used IrDA2 Click [50] as the transceiver. It supports IrDA speeds up to 115.2 Kbit/s. Integrated within the transceiver module are a photo pin diode, an infrared emitter (IRED), and a low-power control IC to provide a total front-end solution in a single package. This device covers the full IrDA range of 3 m using the internal intensity control. The IRED has peak emission wavelength of 900 nm and the angle of half intensity is $\pm 24^\circ$.

5.1.3. Synchronization and message passing

We performed experiments in two scenarios. In one scenario, we kept both nodes (Node A and Node B) stationary. In the other scenario, we kept Node A stationary and Node B mobile. Since the available IrDA2-click transceivers works in half-duplex mode, we considered Node A as the slave and Node B as the master. Node B sends a search signal and Node A keeps listening for it to discover

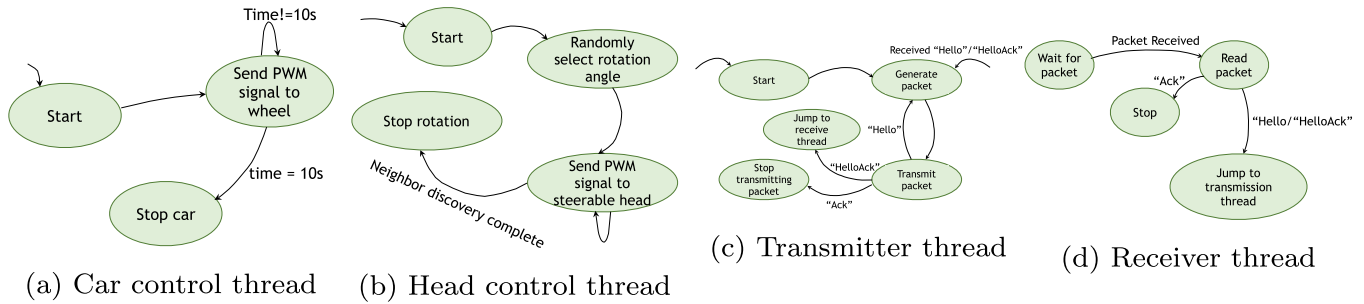


Fig. 17. Different threads running in the prototype.

each other. It is worthy to mention that, in case of full duplex communication, both transceivers can transmit and listen at the same time. Thus, the experiments carried out with this prototype will be valid for full duplex transceivers also.

The two nodes are kept in different random positions but within the communication range of each other's transceivers. We start by launching the programs in the Nodes' Raspberry Pi. This initializes the GPIO pins and configures specific pins to be used as input/output for the various sensors and controller signals. Then, Node A generates three threads: one for head control (Fig. 17b), one for packet transmission and another for packet reception (Fig. 17d). Node B generates three (stationary scenario) or four (mobile scenario) separate threads: one for packet transmission (Fig. 17c), one for packet reception, one for car control (Fig. 17a) and one for head control. The car control thread in Node B periodically sends a PWM signal to the GPIO pins that runs the wheels. The head control thread performs the head rotation. The transmission and reception threads are used for transmitting and receiving packets respectively. Node B continuously rotates its head and sends "Hello" packets. After each "Hello" packet, it listens for an acknowledgment "HelloACK" from neighbor Node A for 50ms. This delay can be reduced but in the prototype, we found it to be optimal with the current set of hardware. The sender waits during this time period for a reply from the receiver. After 50ms, it sends the next "Hello" packet. On the other hand, Node A keeps listening for the "Hello" packet. Upon receiving the "Hello" packet, it responds with a "HelloACK" packet and starts listening again for an acknowledgment "ACK" from Node B. When Node B receives the "HelloACK", it responds with "ACK", stops rotating its head and does not send any more packets (and stops moving if it was mobile). And as soon as this "ACK" is received by Node A, it also stops rotating its head, thus completing the neighbor discovery.

5.1.4. System limitations

The servo motors used to rotate the heads could only perform a 180° rotation. So, we emulated the 181° to 360° rotation by rotating the heads in the opposite direction from 179° to 0° , once it reached 180° . We always kept the nodes within $0^\circ - 180^\circ$ scanning area of each other and made sure they did not transmit or receive packets during the $179^\circ - 0^\circ$ rotation. Also, the data trans-

mission and reception in the two nodes were not solely performed by the Raspberry Pi. We placed an Arduino using the IrDA2 transceiver and the Raspberry Pi. The IrDA2 is connected to an Arduino using an Arduino shield. The Arduino along with the IrDA2 transceiver are mounted on the inner ring of the rotating head. The Arduino is introduced as a buffer between the IrDA chip and the Raspberry Pi's GPIO pins. While building the prototype, we found out that the Raspberry Pi has a hardware glitch when trying to communicate using UART. Every transmitting packet was being preceded by an unintentional high bit. When using the UART directly with the IrDA chip, this unintentional bit was being interpreted as a start signal. The packet being read by the IrDA from the Raspberry Pi was then incorrect. Due to the short duration of the bit, the Arduino does not read the bit as a start bit and ignores the unintentional start bit. By using the Arduino as a buffer between IRDA and the Raspberry Pi, the unintentional start bit is filtered out and the correct packet is transmitted and received through the IR transceivers.

5.2. Experimental results

As the first step, we measure the transmission time needed for the packets. Note that the measured time includes the delay caused by the Arduino board and internal processing time at Raspberry Pi. We took 1000 samples and the average transmission time is measured as $48.44 \mu\text{s}$. The next parameter we measured is the processing time as $1078.73 \mu\text{s}$. The processing times varies heavily with the working load on the Raspberry Pi. This delay can be significantly reduced using a newer version of the Raspberry Pi that provides higher processing power. We conducted experiments in two different setups: 1) the nodes are static and 2) one of the nodes is moving. In the subsequent sections, we describe the experiment results.

5.2.1. Static scenario

Fig. 18 provides a snapshot of the experiment. In the figures, we have depicted the transceivers with imaginary gain patterns for better visualization. Nodes A and B are placed at random positions and are unaware of each other's position. Their transceivers are randomly oriented at the start, as can be seen in Fig. 18(a).

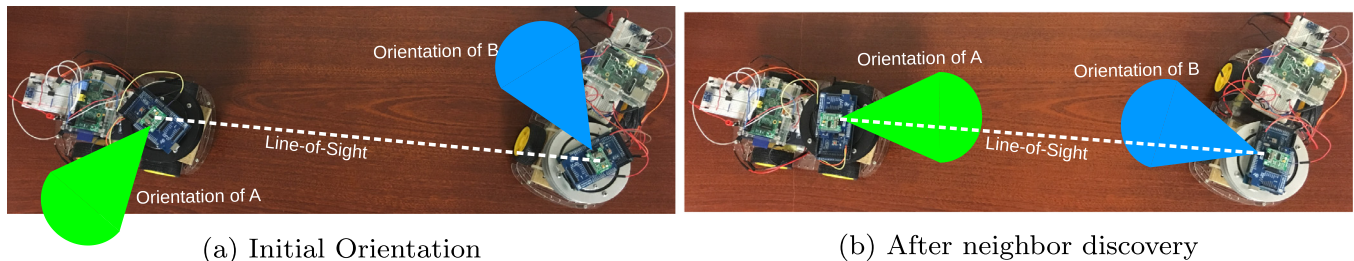


Fig. 18. A snapshot of the experiment.

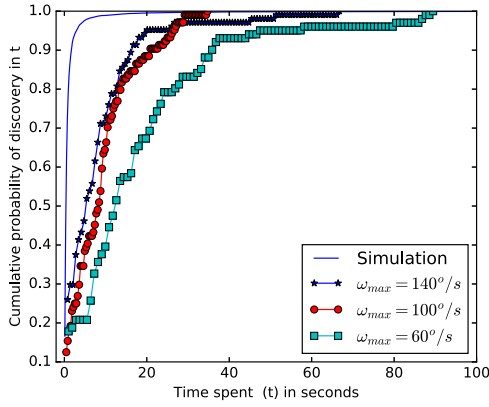


Fig. 19. CDF of discovery within time t for experiments with the prototype with different maximum rotation speed.

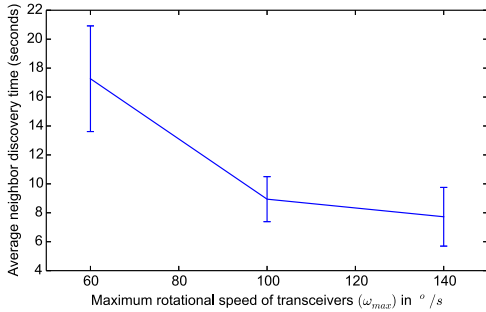


Fig. 20. Average neighbor discovery time for the prototype while varying the maximum rotational speed.

Then they follow the neighbor discovery algorithm described in Algorithm 1 with an exception. In the algorithm, each node chooses an angular speed ω , from the optimal values (Section 3.3). Unfortunately, the steerable head of our prototype can not support such high speed. So, in the experiments, it chooses $\omega \in (0, 140^\circ/s]$. After the successful neighbor discovery, both nodes stop rotating their heads, and the orientation after discovery LOS can be seen in Fig. 18(b).

In this experimental setup, the transceivers nodes are kept at a distance of 2m. We repeated the experiment 100 times to obtain reliable results. During each run of the experiment, the nodes choose their initial head orientations randomly. Since the maximum ideal rotational speed ω_{max} , as in Algorithm 1, can not be obtained by the prototype, We conducted the experiment for three feasible values of ω_{max} : $60^\circ/s$, $100^\circ/s$ and $140^\circ/s$. Fig. 19 provides the cumulative probability of discovery within time t . It can be seen that, the discovery time taken is very large compared to the ideal simulation. This limitation is due to that fact that the transceiver head does not rotate with the desired speed. The speed also varies with the battery power. We can also observe that, the probability of neighbor discovery increases with increase in the maximum rotational speed (ω_{max}) of the transceiver heads. Again, from Fig. 20, can clearly see that with a higher rotational speed, the nodes can discover each other faster. However, despite the limitation of head rotational speed, on average the nodes can discover each other within $\approx 8.53s$.

5.2.2. Mobile scenario

In this setup, we tested the feasibility of the proposed neighbor discovery method for mobile nodes. The test arena is depicted in Fig. 21. One node is stationary, while the other moves as can be seen in the prototype video [45]. Both nodes follow the neighbor discovery protocol described earlier with the limitation that the

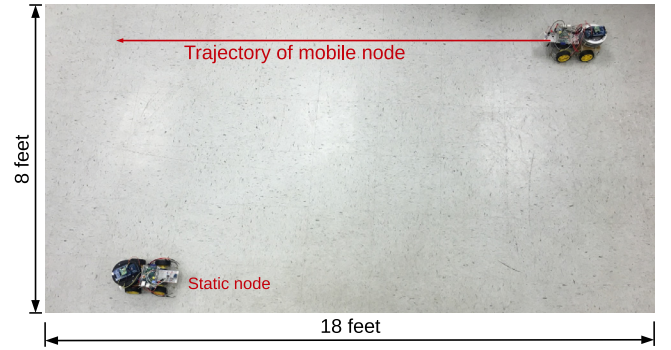


Fig. 21. Setup for Experiments with mobile node.

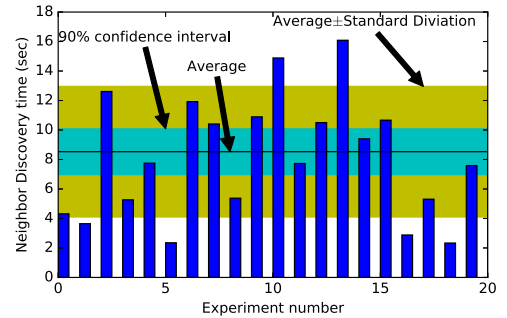


Fig. 22. Experiment results for mobile nodes. Here the bars indicate the time taken for discovery for each experiment. The yellow and cyan regions indicate the standard deviation and the 90% confidence intervals respectively.

transceivers can rotate with a maximum angular speed of $140^\circ/s$. In this experiment, the mobile node stops moving after the 3-way handshake is complete. Since the nodes are unaware of the neighbor's location, they start with a random initial orientation. The discovery time is measured as the time between the start of the search operation of the mobile node and the completion of the three-way handshake.

Fig. 22 displays the discovery times achieved from the conducted experiments. The X axis denotes the particular experiment number, and the bar length or Y axis indicates the time taken for discovery. The average time for discovery is measured as 8.52s. The standard deviation is calculated as 4.43. In Fig. 22, the cyan region indicates the 90% confidence interval of the neighbor discovery time.

6. Conclusion

We proposed a novel approach for discovering neighbors via line-of-sight (LOS) directional links in both stationary and mobile scenarios. We assumed that, the nodes do not have any prior information about their neighbors' locations. We considered nodes equipped with a mechanically steerable head/arm on which a highly directional FSO or RF transceiver is mounted. There is no other additional omnidirectional communication link available to the nodes. The nodes rotate the transceivers and send search signals to discover the neighbors. We proposed a method for finding optimal rotational speeds for the node's heads mounted with transceivers. Through extensive simulations and real prototype experiments, we showed that the nodes could discover each other within a reasonable period of time. We also evaluated how the directional neighbor discovery protocol would perform when there are multiple neighbors. A possible line of future work is to solve the problem in 3D and consider a ground-to-air link or LOS

discovery between two airborne mobile nodes using directional FSO or RF transceivers.

Conflict of interest

None declared.

References

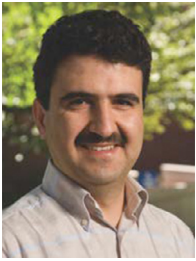
- [1] S. Bhunia, M. Khan, S. Sengupta, M. Yuksel, Los discovery for highly directional full duplex RF/FSO transceivers, in: Proceedings of the Military Communications Conference (MILCOM), 2016.
- [2] R.R. Choudhury, X. Yang, R. Ramanathan, N.H. Vaidya, Using directional antennas for medium access control in ad hoc networks, in: Proceedings of the International Conference on Mobile Computing and Networking, ACM, 2002, pp. 59–70.
- [3] R. Ramanathan, J. Redi, C. Santivanez, D. Wiggins, S. Polit, Ad hoc networking with directional antennas: a complete system solution, *IEEE JSAC* 23 (3) (2005) 496–506.
- [4] R.R. Choudhury, X. Yang, R. Ramanathan, N.H. Vaidya, On designing MAC protocols for wireless networks using directional antennas, *IEEE Trans. Mob. Comput.* 5 (5) (2006).
- [5] Z. Zhang, B. Li, Neighbor discovery in mobile ad hoc self-configuring networks with directional antennas: algorithms and comparisons, *IEEE Trans. Wirel. Commun.* 7 (5) (2008) 1540–1549.
- [6] S. Bhunia, V. Behzadan, P.A. Regis, S. Sengupta, Adaptive beam nulling in multi-hop ad hoc networks against a jammer in motion, *Comput. Netw.* (2016), doi:10.1016/j.comnet.2016.06.030.
- [7] S. Bhunia, V. Behzadan, P.A. Regis, S. Sengupta, Performance of adaptive beam nulling in multi-hop ad-hoc networks under jamming, in: Proceedings of the IEEE CSS, 2015.
- [8] S. Bhunia, S. Sengupta, Distributed adaptive beam nulling to mitigate jamming in 3D UAV mesh networks, in: Proceedings of the ICNC, 2017.
- [9] A. Sevincer, A. Bhattarai, M. Bilgi, M. Yuksel, N. Pala, Lightnets: smart lighting and mobile optical wireless networks survey, *IEEE Commun. Surv. Tutor.* 15 (4) (2013).
- [10] Facebook laser communication. <https://www.facebook.com/zuck/video/10102274951725301/>.
- [11] M. Khan, M. Yuksel, G. Winkelmanier, Gps-free maintenance of a free-space-optical link between two autonomous mobiles, *IEEE Trans. Mob. Comput.* (1) (2015), 1–1.
- [12] E. Everett, M. Duarte, C. Dick, A. Sabharwal, Empowering full-duplex wireless communication by exploiting directional diversity, in: Proceedings of the ASILOMAR, IEEE, 2011, pp. 2002–2006.
- [13] D. Bharadia, E. McMillin, S. Katti, Full duplex radios, in: Proceedings of the ACM SIGCOMM, 2013, pp. 375–386.
- [14] E. Everett, A. Sahai, A. Sabharwal, Passive self-interference suppression for full-duplex infrastructure nodes, *IEEE Trans. Wirel. Commun.* 13 (2) (2014) 680–694.
- [15] M. Duarte, C. Dick, A. Sabharwal, Experiment-driven characterization of full-duplex wireless systems, *IEEE Trans. Wirel. Commun.* 11 (12) (2012) 4296–4307.
- [16] M. Duarte, A. Sabharwal, V. Aggarwal, R. Jana, K. Ramakrishnan, C.W. Rice, N. Shankaranarayanan, Design and characterization of a full-duplex multi-antenna system for WIFI networks, *IEEE Trans. Veh. Technol.* 63 (3) (2014) 1160–1177.
- [17] R. Sun, D.W. Matolak, Over-harbor channel modeling with directional ground station antennas for the air-ground channel, in: Proceedings of the IEEE MILCOM, 2014.
- [18] J. Chen, J. Xie, Y. Gu, S. Li, S. Fu, Y. Wan, K. Lu, Long-range and broadband aerial communication using directional antennas (ACDA): design and implementation, *IEEE Trans. Veh. Technol.* 66 (12) (2017) 10793–10805.
- [19] A. Jalali, Broadband access system via drone/UAV platforms, 2017. US Patent 9,853,715.
- [20] A. Jalali, Apparatus and methods to provide communications to aerial platforms, 2018. US Patent App. 15/456,233.
- [21] D. Zahavi, S.B. Laufer, Large aperture antenna with narrow angle fast beam steering, 2017. US Patent 9,812,775
- [22] A.A. Artemenko, V.N. Ssorin, R.O. Maslennikov, A.V. Mozharovskiy, Lens antenna with electronic beam steering capabilities, 2015. US Patent App. 14/593,552.
- [23] irobot. <http://www.irobot.com/us/learn/defense/packbot>.
- [24] Nasa k10 robots. <http://www.nasa.gov/centers/ames/K10/>.
- [25] Y. Wang, S. Mao, T.S. Rappaport, On directional neighbor discovery in mmWave networks, in: Proceedings of the ICDCS, 2017.
- [26] R.W. DeVaul, E. Teller, C.L. Biffle, J. Weaver, Establishing optical-communication lock with nearby balloon, 2012. US Patent App. 13/346,645
- [27] R. DeVaul, E. Teller, C. Biffle, J. Weaver, Using predicted movement to maintain optical-communication lock with nearby balloon, 2013. US Patent App. 14/108,542
- [28] M. Khan, M. Yuksel, Autonomous alignment of free-space-optical links between UAVs, in: Proceedings of the Second International Workshop on Hot Topics in Wireless, ACM, 2015, pp. 36–40.
- [29] K. Wang, A. Nirmalathas, C. Lim, E. Skafidas, Experimental demonstration of full-duplex optical wireless personal area communication system with 16-cap modulation, in: Proceedings of the Optical Fiber Communications Conference and Exhibition (OFC), 2015, IEEE, 2015, pp. 1–3.
- [30] K. Wang, A. Nirmalathas, C. Lim, K. Alameh, E. Skafidas, Full-duplex gigabit in-door optical wireless communication system with cap modulation, *IEEE Photonics Technol. Lett.* 28 (7) (2016) 790–793.
- [31] B.E. Johnson, T.A. Lindsay, D.L. Brodeur, R.E. Morton, M.A. Regnier, Wide-angle, high-speed, free-space optical communications system, 1994. US Patent 5,359,446.
- [32] A. Sevincer, M. Bilgi, M. Yuksel, Automatic realignment with electronic steering of free-space-optical transceivers in MANETS: a proof-of-concept prototype, *Ad Hoc Netw.* 11 (1) (2013).
- [33] P. Zhang, Y. Lou, T. Wang, G. Yang, L. Zhang, S. Tong, H. Jiang, Link budget and simulation of double-wavelength full-duplex free-space laser communication based on modulating retro-reflector, *Wireless Communications, Networking and Applications*, Springer, 2016.
- [34] E.J. Mayeux, Optical transceiver for free-space communication links, 1995. US Patent 5,390,040.
- [35] X. Xie, X. Zhang, Does full-duplex double the capacity of wireless networks? in: Proceedings of the INFOCOM, IEEE, 2014.
- [36] S. Goyal, P. Liu, O. Gurbuz, E. Erkip, S. Panwar, A distributed mac protocol for full duplex radio, in: Proceedings of the Conference on Signals, Systems and Computers, 2013 Asilomar, IEEE, 2013, pp. 788–792.
- [37] X. An, R. Hekmat, Self-adaptive neighbor discovery in ad hoc networks with directional transceivers, in: Proceedings of the Sixteenth IST Mobile and Wireless Communications Summit, 2007, IEEE, 2007, pp. 1–5.
- [38] Z. Zhang, Performance of neighbor discovery algorithms in mobile ad hoc self-configuring networks with directional antennas, in: Proceedings of the IEEE MILCOM 2005, 2005, pp. 3162–3168.
- [39] G. Pei, M.M. Albuquerque, J.H. Kim, D.P. Nast, P.R. Norris, A neighbor discovery protocol for directional antenna networks, in: Proceedings of the IEEE MILCOM, IEEE, 2005, pp. 487–492.
- [40] M. Khan, S. Bhunia, M. Yuksel, S. Sengupta, Los discovery in 3d for highly directional transceivers, in: Proceedings of the Military Communications Conference (MILCOM), 2016.
- [41] S. Vasudevan, J. Kurose, D. Towsley, On neighbor discovery in wireless networks with directional antennas, in: Proceedings of the IEEE INFOCOM, 2005.
- [42] G. Jakllari, W. Luo, S.V. Krishnamurthy, An integrated neighbor discovery and MAC protocol for ad hoc networks using directional antennas, *IEEE Trans. Wirel. Commun.* 6 (3) (2007) 1114–1024.
- [43] L. Chen, Y. Li, A.V. Vasilakos, On oblivious neighbor discovery in distributed wireless networks with directional antennas: theoretical foundation and algorithm design, *IEEE/ACM Trans. Netw.* 25 (4) (2017) 1982–1993, doi:10.1109/TNET.2017.2673862.
- [44] M. Khan, M. Yuksel, Maintaining a free-space-optical communication link between two autonomous mobiles, proceedings of the IEEE WCNC, 2014.
- [45] Prototype video, (http://sbhunias.me/research/neighbor_discovery/).
- [46] M. Khan, G. Winkelmanier, M. Yuksel, In-band autonomous maintenance of mobile free-space-optical links: a prototype, in: Proceedings of the IEEE ICC, 2016.
- [47] Raspberry Pi. <https://www.arduino.cc/en/reference/servo>.
- [48] Emgreat 4-wheel robot smart car. <http://www.amazon.com/Emgreat-4-wheel-Chassis-Encoder-Arduino/>.
- [49] Aluminium robot turntable swivel base. <http://www.ebay.com/itm/Aluminium-Robot-Turntable-Swivel-Base-2-DOF-PTZ-2pcs-Servo-Set-for-Arduino-/271254609757>.
- [50] IrDA2 click. <http://www.mikroe.com/click/irda2/>.



Suman Bhunia is a postdoctoral scholar at the Texas A&M University, College Station. He obtained his Ph.D. in Computer Science from the University of Nevada, Reno in 2017. He earned a bachelors degree in Electronics and Communication Engineering in 2008 from the West Bengal University of Technology and a masters degree in Distributed and Mobile Computing in 2010 from Jadavpur University, India. His research area is security and vulnerabilities in wireless communications.



Mahmudur Khan received the B.Sc. degree in electrical and electronic engineering from the Bangladesh University of Engineering and Technology in 2011 and the M.S. degree in computer science and engineering from the University of Nevada Reno in 2015. He received the Ph.D. degree in computer engineering from the University of Central Florida in 2018. He is a post-doctoral researcher in the ECE department at The University of Alabama. His research interests include the area of free-space-optical communications, wireless ad hoc networks, and UAV communications. He is a member of the IEEE.



Murat Yuksel received the BS degree in computer engineering at Ege University, Izmir, Turkey, in 1996, and the MS and Ph.D. degrees in computer science from RPI in 1999 and 2002, respectively. He is an associate professor in the ECE Department at the University of Central Florida (UCF), Orlando, FL. Prior to UCF, he was with the CSE Department at the University of NevadaReno (UNR), Reno, NV, as a faculty member until 2016. He was with the ECSE Department at the Rensselaer Polytechnic Institute (RPI), Troy, NY, as a postdoctoral associate and a member of adjunct faculty until 2006. He worked as a software engineer at Pepperdata, Sunnyvale, CA and a visiting researcher at AT&T Labs and Los Alamos National Lab. His

research interests are in the area of networked, wireless, and computer systems with a recent focus on big-data networking, UAV networks, optical wireless, public safety communications, device-todevice protocols, economics of cyber-security and cybersharing, routing economics, network management, and network architectures. He has been on the editorial board of Computer Networks, and published more than 100 papers in peer-reviewed journals and conferences and is a corecipient of the IEEE LANMAN 2008 Best Paper Award. He is a senior member of the IEEE, and a senior and life member of the ACM.



Shamik Sengupta is an Associate Professor in the Department of Computer Science and Engineering at University of Nevada, Reno (UNR). Dr. Sengupta received his Ph.D. degree from the School of Electrical Engineering and Computer Science, University of Central Florida in 2007. Prior to that, he completed his B.E. degree (First class with Hons.) in Computer Science & Engineering from Jadavpur University, India in 2002. Before joining University of Nevada, Reno, Dr. Sengupta worked as a Post-Doctorate Researcher at Stevens Institute of Technology and an Assistant Professor at City University of New York (John Jay College of Criminal Justice). He is a recipient of the NSF CAREER award. He has also held visiting researcher posi-

tion at AFRL, Rome, NY.